

# UC San Diego

## UC San Diego Previously Published Works

### Title

Circuit mechanisms of hippocampal reactivation during sleep

### Permalink

<https://escholarship.org/uc/item/9450r94f>

### Authors

Malerba, Paola  
Bazhenov, Maxim

### Publication Date

2019-04-01

### DOI

10.1016/j.nlm.2018.04.018

Peer reviewed



Published in final edited form as:

*Neurobiol Learn Mem.* 2019 April ; 160: 98–107. doi:10.1016/j.nlm.2018.04.018.

## Circuit mechanisms of hippocampal reactivation during sleep

Paola Malerba<sup>1</sup>Maxim Bazhenov\*

Department of Medicine, University of California San Diego, United States

### Abstract

The hippocampus is important for memory and learning, being a brain site where initial memories are formed and where sharp wave – ripples (SWR) are found, which are responsible for mapping recent memories to longterm storage during sleep-related memory replay. While this conceptual schema is well established, specific intrinsic and network-level mechanisms driving spatio-temporal patterns of hippocampal activity during sleep, and specifically controlling off-line memory reactivation are unknown. In this study, we discuss a model of hippocampal CA1-CA3 network generating spontaneous characteristic SWR activity. Our study predicts the properties of CA3 input which are necessary for successful CA1 ripple generation and the role of synaptic interactions and intrinsic excitability in spike sequence replay during SWRs. Specifically, we found that excitatory synaptic connections promote reactivation in both CA3 and CA1, but the different dynamics of sharp waves in CA3 and ripples in CA1 result in a differential role for synaptic inhibition in modulating replay: promoting spike sequence specificity in CA3 but not in CA1 areas. Finally, we describe how awake learning of spatial trajectories leads to synaptic changes sufficient to drive hippocampal cells' reactivation during sleep, as required for sleep-related memory consolidation.

### Keywords

Sharp-wave ripples; Replay; Sleep-dependent memory consolidation

## 1. Introduction

Sleep-mediated memory consolidation is the process by which the brain reinforces selective memories acquired during the day, rendering them resilient to interference from what we learn in future days. While the hippocampus quickly stores information on daily events, sleep represents a concerted brain-wide effort in which the dialogue of hippocampus and cortex mediates memory consolidation. Consolidation is selective (Feld et al., 2016; Ellenbogen et al., 2006; McDevitt et al., 2015)), integrative (new memories are embedded in the personal narrative and knowledge (Rasch & Born, 2013)) and progressive (the memory processing continues for hours to years (Diekelmann & Born, 2010)). This very layered and complex brain function is tied to some characteristic brain rhythms, particularly those found during Non-Rapid Eye Movement (NREM) sleep, which cover a range of regions,

\*Corresponding author at: University of California San Diego, Department of Medicine, 9500 Gilman Drive # 7381, La Jolla, CA 92037, United States., mbazhenov@ucsd.edu (M. Bazhenov).

<sup>1</sup>Present address: Department of Cognitive Sciences, University of California Irvine, United States.

frequencies and time scales (Rasch & Born, 2013): slow oscillations in cortex (0.2–1.5 Hz, lasting from a few cycles to minutes of oscillations), cortico-thalamic spindles (9–16 Hz, each event lasting 0.5–3 s) and hippocampal sharp-wave ripples (150–250 Hz, each event lasting 60–100 ms). This rhythmic orchestra is found to play during sleep in an organized manner, where the slowest rhythm (slow oscillations) modulates the occurrence probability of the intermediate rhythm (spindles) and in turn the coordination of slow oscillations and spindles modulates the occurrence of hippocampal ripples (Latchoumane, 2017; Molle & Born, 2011; Rasch & Born, 2013; Sirota et al., 2003; Staresina, 2015). The differential neurotransmitter levels that characterize sleep are thought to play a role in facilitating the generation of these oscillations, in particular hippocampal ripples (Atherton et al., 2015; Buzsaki et al., 1983; Hasselmo, 1999; Vandecasteele, 2014). The known connections between these rhythms and memory consolidation include: (a) increased power of slow oscillation, e.g., by auditory cues or electrical stimulation during sleep, enhances memory performance (Marshall, 2006; Ngo, 2013; Ngo, 2013), (b) intense learning increases the number of spindles found during sleep (Studte et al., 2017), and (c) disrupting ripples impairs memory consolidation (Ego-Stengel & Wilson, 2010; Girardeau, 2009). Furthermore, cell sequence replay, a phenomenon in which cells active during the task reactivate during sleep preserving their firing order, happens in the hippocampus during sharp waveripple (SWR) events, and in cortex during the active parts of the slow oscillation (called Up states) (Foster & Wilson, 2006; Hoffman & McNaughton, 2002; Ji & Wilson, 2007; Schwindel & McNaughton, 2011; Skaggs & McNaughton, 1996; Sutherland & McNaughton, 2000; Wilson & McNaughton, 1994; Wu & Foster, 2014). One leading hypothesis is that sleep dependent consolidation happens due to coordinated reactivation of cell sequences across hippocampus and cortex, which enables appropriate synaptic plasticity, and that sleep rhythms and precise coordination between them are crucial for this organized hippocampo-cortical activation to occur (Mehta, 2007).

As part of the question of how is memory consolidation performed by the brain during sleep, understanding the specific mechanisms that shape the emergence of hippocampal SWRs and the sequence replay within them, is essential. Indeed, when experimental interventions impose the presence of a cell spiking sequence within SWR, they can engineer a new memory (Liu, 2012; Ramirez et al., 2013; Ramirez, 2013) and when the content of SWR replay is damaged, so is the memory performance after sleep (Ego-Stengel & Wilson, 2010; Girardeau, 2009). In this work, we show how a relatively simple biophysical model of activity in CA3 and CA1 can offer insights on the dynamics of sharp waves in CA3 and ripples in CA1, and particularly on how reactivation in CA3 and CA1 is shaped by different emergent mechanisms. We then show how a model of a “virtual rat” exploring an environment and learning one trajectory can be used to theorize on the relationship between plasticity during learning and spontaneous reactivation during sleep, in particular emphasizing how to learn a new memory it is crucial to choose which cells can encode for it in relation to the pre-existing coding structure already built. Any new learning always takes place on the background of existing memories, so it is a continuous process of integration and refining of synaptic architecture. Effective hippocampal sleep replay of novel information requires encoding of such information during learning that takes into account what is already learned (Grosmark & Buzsaki, 2016).

## 2. Results

### 2.1. How are ripples generated in CA1?

Hippocampal sharp-wave ripples involve two different sub-regions, areas CA3 and CA1. In fact, they are commonly referred to as SWR complexes. While the activation in CA1 and CA3 during SWR complexes is closely related, it is also known to have different properties among the two regions at the level of single unit activity and LFP (Csicsvari, 2000; Csicsvari et al., 1999; Mizuseki, 2012; Sullivan, 2011). In this work, we are going to refer to sharp waves as the activity in CA3 which contributes to a SWR complex, and to ripples as the activity in CA1 which contributes to a SWR complex. Sharp waves are short-lived bouts of intense excitatory spiking which invade area CA3 and drive spiking of excitatory and inhibitory neurons in area CA1. Recordings of local field potentials (LFP) in area CA1 show that when CA3 sharp-wave inputs arrive, a high-frequency oscillation – ripple event - is developed in the CA1 pyramidal layer (Buzsaki, 2003, 2015; Csicsvari, 2000; Gan, 2017). The mechanism that makes a ripple appear in the presence of a CA3 sharp wave has been investigated *in vitro* (Kubota, 2003; Maier et al., 2003; Maier, 2009; Schlingloff, 2014) and *in vivo* (Buzsaki, 2003; English et al., 2014; Oliva, 2016; Patel, 2013; Stark, 2014; Ylinen, 1995), and a number of computational studies have attempted modeling of CA1 ripples, either focusing on the role of electric coupling (known as gap junctions) between hippocampal pyramidal cells in generating and propagating a ripple (Draguhn, 1998; Traub & Bibbig, 2000; Traub, 1999), or suggesting a predominant role of more-than linear synaptic potentiation of the few and rare synaptic connections among pyramidal cells in CA1 (Jahnke et al., 2015; Memmesheimer, 2010). A different approach looks at CA1 ripples as their own local oscillation triggered by incoming CA3 excitation (Cutsuridis & Taxis, 2013; Ellender, 2010; Taxis, 2012), in which inhibitory synaptic connections are responsible for the oscillations in CA1, the latter can be called interneuron-based models of ripples.

In our recently proposed model of ripple generation in the presence of CA3 input (Malerba, 2016), ripples are not persistent oscillations but rather emerge from a short-lived transient network behavior, driven by highly synchronous input onset. This newly designed ripple mechanism suggests that CA1 basket cells do fire at high frequency pacing the ripple (Fig. 1A) but do not coordinate via their reciprocal inhibition. Instead, their initial coordination is due to the strong incoming CA3 input, and noise-induced phase dispersion dynamically constrains ripple duration (Fig. 1B). Local CA1 inhibition then selects which CA1 pyramidal cells get an opportunity to spike (replay) in a given ripple event. This model shows strong agreement with the *in vivo* results of Stark (2014), where optogenetic stimulation was used to drive spiking in the populations of basket cells and pyramidal cells together and separately; this study predicted that to observe a ripple in the CA1 LFP, input to both pyramidal and basket cells is necessary. In fact, the strong inhibitory transient in basket cells initiated by input (either from a CA3 sharp wave or from optical drive) will suppress pyramidal cell activity in CA1, resulting in a shunted CA1 LFP, if pyramidal cells were not excited by the same input.

## 2.2. Role of CA3 in generation of sharp-wave ripple complexes

For a CA1 ripple to occur a CA3 sharp wave is required. While CA1 ripples have a distinct high-frequency signature and show locked spiking to the LFP in excitatory and inhibitory populations, activity in CA3 during a sharp wave is characterized by intense pyramidal and basket cell spiking, seems to be strongly related to the topology of recurrent connections between CA3 pyramidal cells, and does not show locking to CA1 ripples (Csicsvari, 2000; Csicsvari et al., 1999; Sullivan, 2011). Computational models of CA3 sharp wave activity have suggested either a role of gap junctions in initiating and propagating the activity (Draguhn, 1998; Traub & Bibbig, 2000; Traub, 1999) or emphasized the role of the variance in the strength of synaptic connections between pyramidal cells (Omura, 2015). In general, it is agreed that recurrent CA3 pyramidal cells connectivity is important if not crucial for CA3 sharp waves to emerge in the network activity.

Here we propose a novel model of CA3-CA1 sharp-wave ripples (Fig. 2), extending our previous model of ripple generation in CA1 (Malerba, 2016) to hippocampal areas CA3 and CA1. This model shows spontaneously occurring large CA3 excitatory events (the CA3 sharp waves) driving rhythmic spiking in CA1 interneurons (the CA1 ripples), which give the combined sharp-wave ripple complexes. CA3 activity emerged spontaneously and triggered stochastic activation of SWR complexes in CA3 and CA1 combined, with the termination of CA1 ripples driven by the same de-coordination mechanism as in the CA1 model. In this new model of CA3-CA1 SWR complexes, different subsets of neurons in both CA3 and CA1 participated in different SWR events (Fig. 2A) as observed experimentally (Patel, 2013). This model of CA3-CA1 SWR complex activity was based on synaptically coupled populations of pyramidal cells and basket cells (Fig. 2A). It included highly recurrent strong excitatory AMPA receptor-mediated connections between CA3 pyramidal cells, and weak and sparse recurrent excitatory connections within CA1 pyramidal cells (Shepherd, 2004). CA3 pyramidal cells projected excitatory connections to CA1 cells, representing the Schaffer Collaterals. The CA3 network and its projections to CA1 had stochastic densities and strengths within a radius of about a third of the target network, which is consistent with experimental analysis of CA3 pyramidal cells arborization (Li, 1994). Importantly, each neuron received an independent noise current which drove occasional irregular spiking, and a baseline constant drive which was selected from a Gaussian distribution. Details of the computational model rationale and equations are reported in Materials and Methods.

As shown in Fig. 2A, the CA3 network spontaneously organized into bouts of pyramidal cell spiking, which drove spiking events in CA1. As a result, CA1 interneurons organized their firing into high frequency oscillations, and a few pyramidal cells spiked within windows of opportunity left at the troughs of the lateral synaptic inhibition oscillations, thus forming a SWR complex event across the combined CA3-CA1 network. As *in vivo* (Davidson et al., 2009), SWR complexes occurred in temporal clusters punctuated by long pauses. A representation of the LFP in the model obtained by averaging the synaptic currents impinging on subsets of pyramidal cells showed that combined SWR events in CA3 and CA1 were localized, and the location of the SWRs within the CA3-CA1 network changed in time (Fig. 2A). This is consistent with experimental findings showing that CA1 ripple events

can be localized in space (Patel, 2013; Ylinen, 1995) and that CA3 pyramidal cells are known to be very active during SWR, but do not spike phase-locked to CA1 ripples (Atherton et al., 2015; Sullivan, 2011). The general activity of the model was consistent with known properties of SWR complexes: ripple frequency was  $174 \pm 21.3$  Hz, ripple durations were  $54 \pm 27$  ms, sharp wave durations were  $126 \pm 23$  ms and the interevent pauses (time durations between two successive sharp waves in CA3 or ripples in CA1) showed approximately exponential distributions, which fitted to exponential functions with rates of 1.08 Hz in CA3 and 1.2 Hz in CA1 (Buzsaki, 2015).

Spiking of the excitatory and inhibitory populations in CA3 and CA1 in our model revealed the fundamentally different dynamics in the two regions: with CA3 activity characterized by similar spiking (initiated by pyramidal cells) in the excitatory and inhibitory populations, while CA1 ripples were primarily inhibitory events where few pyramidal cells find small windows of opportunity to spike (Fig. 2B and C). This is evident when activity in a region (either CA3 or CA1) was measured by either the fraction of a cell population spiking during an event (CA3 sharp wave or CA1 ripple, respectively) (Fig. 2B) or by the number of spikes that each neuron shows during the event (Fig. 2C).

Despite the difference in the dynamics of sharp wave and ripples, the model captured the interaction between CA3 and CA1 patterns of activity during SWRs, which coordinated and modified their locations, timing and size when network connectivity was rearranged (Fig. 3). To test how CA3 activity is reflected on CA1 activity, we used a parameter which controls the density of the recurrent connectivity within CA3 pyramidal cells and of Schaffer Collaterals projections on CA1 pyramidal cells ( $k$ , see Section 6). Larger  $k$  values corresponded to less dense and more broadly distributed excitatory connections, and viceversa smaller  $k$  values resulted in more narrow and denser excitatory input convergence (Fig. 3A and B). Since SWRs in our model involved only ever-changing portions of the whole pyramidal cell population, we could mark a sharp wave location in CA3 by finding which cells were spiking in the event (and the same for CA1 ripples). For each different network organization (i.e.  $k$  value) we observed that the location of CA3 sharp waves changed: from more central and fixed in time for the most dense and narrow recurrence (i.e. the lowest  $k$ ) considered, to distributed uniformly across most of the network in the less dense recurrence (largest  $k$ ) condition (Fig. 3C). This pattern, from more concentrated and fixed to more distributed and varying, was mirrored in the CA1 network when we looked at the ripple locations (Fig. 3D). Changes in CA3 sharp wave activity were hence reflected in changes of CA1 ripples.

Overall, both the data and the model dynamics suggest that sharp wave and ripples are different dynamical objects which interact and depend on each other. Importantly, however, *in vivo* not all sharp wave-like events in CA3 dynamics are matched by a CA1 ripple (; Csicsvari et al., 1999; Sullivan, 2011) [. This leads to the question what properties of sharp waves in CA3 determine the likelihood of successful ripple event in CA1. Indeed, our model revealed the spontaneous occurrence of “failed” sharp waves: excitatory events in CA3 that could not induce ripples in CA1. To quantify the properties of successful vs failed SPW events, the following procedure was applied. We first detected putative sharp wave events in CA3 activity by thresholding on the ongoing CA3 pyramidal cell population spiking activity

(peaks higher than 1std above baseline are putative SPWs). We then looked at the ongoing CA1 activity in response to such inputs, and checked if a ripple was triggered by the putative SPW event. If no ripple was found, we labeled the SPW “failed”, otherwise “successful”. When comparing activity in CA3 during successful vs failed sharp waves, we found that they could be similar in the fraction of cell spiking during the events (in some sense their “size”, how many cells were spiking at all), but that the synchronicity of excitatory firing during a sharp wave was the property best predicting successful sharp waves vs. failing ones. This fact is illustrated in the comparison between Fig. 4A and B: in each panel we show the probability density of event size and synchronicity of either a successful (panel A) or failed (panel B) sharp wave; scaled within its own group. This means that if there were a ripple event in CA1, most often the corresponding sharp wave activity in CA3 would show high synchrony and about 35% of pyramidal cells spiking (Fig. 4A, red<sup>2</sup> region). CA3 sharp wave events showing high peak synchrony ( $> 1$ ) could be relatively rare (Fig. 4A, lighter blue area) but they always triggered CA1 ripples (dark blue in the corresponding region in Fig. 4B). At the same time, if CA3 sharp wave event did not trigger a ripple in CA1, then most likely this CA3 event showed low synchrony and about 15–20% pyramidal cells spiking (Fig. 4B, red region).

In summary, we found that highly synchronous SPWs in the CA3 area never failed to trigger a ripple even if they were not necessarily the most common type of SPW in the spectrum of the CA3 activity. On the other hand, for CA3 events which show very low synchrony and low size, an event would very rarely lead to a ripple, regardless of how often such events actually happened in the CA3 area. We conclude from this observation that our model shows a nonlinear threshold in the mapping of CA3 sharp waves on CA1 ripple activity. The dynamic gating of CA3 sharp waves by CA1 ripple has a functional implication: potentially this mechanism can contribute to how the hippocampus “decides” what content of CA3 activity should be consolidated (and hence broadcasted to cortex via ripple activity) and what should not, but this is a topic for further investigation.

### 2.3. Role of CA3 input in sequence replay during SWR complexes

The importance of understanding SWR dynamics lies in their crucial role in memory formation and consolidation. To date, the mechanisms underlying sequence reactivation during SWRs (one of the possibly essential components of the process of memory consolidation) are not known. One hypothesis is that input-driven partial reactivation in CA3 can induce pattern completion within the highly recurrent CA3 network, which in turns drives a refined CA1 spike reactivation to be broadcasted to cortex.

We next used our model of CA3-CA1 SWR complexes to explore the relationship between spontaneously emerging cell pair activation during SWRs and the properties of the cells within such a pair (a cell pair being the simplest building block of a cell spiking sequence). To make predictions on which properties can determine the probability of reactivation in two pyramidal cells which are not necessarily directly connected, we considered both synaptic inputs and intrinsic excitability. Specifically, in our analysis, a pair is defined as two cells

---

<sup>2</sup>For interpretation of color in Fig. 4, the reader is referred to the web version of this article.

spiking together in specific order during many SWR. We studied pairs of CA3-CA3 and CA1-CA1 cells, and quantified inputs to the cell pairs differently depending on the hippocampal regions involved, but in all cases we considered the role of excitatory synaptic input, inhibitory synaptic input and intrinsic excitability of either one of the cells in the pair.

We first measured the degree of co-activation of a cell pair as the fraction of the SWR events in which both cells in the pair spiked in the correct order (we called it R-activation score), and tested all possible cell pairs in the CA3 network. For each cell pair, we also found the total excitatory input shared by the cells in the pair by finding all pyramidal cells which projected to both cells in the pair and multiplying the synaptic weights of such connections (Fig. 5A, left panel). We proceeded analogously for shared inhibitory connections, and used a parameter regulating the mean membrane voltage of each cell as a proxy for the intrinsic excitability of the cell. Hence, for each possible ordered cell pair, we had collected (1) a value of the excitatory connection strengths shared by the pair, (2) a value of the inhibitory connection strengths shared by the pair and (3) two values of intrinsic excitability (one for the first cell in the pair, labeled “A” in Fig. 5A, and one for the second – or “B” – cell in the pair). The average (across all pairs) value of each of these different properties was calculated for each range ( $\pm 5\%$ ) of the R-activation score to plot the distributions (Fig. 5A, right panel). We found that CA3-CA3 pairs of neurons that spiked more often together during SPWs tended to have (a) higher amount of shared excitatory and inhibitory inputs; (b) higher intrinsic excitability of the first cell in the pair; (c) lower intrinsic excitability of the second cell in the pair. While it is intuitive that common synaptic excitation could promote co-spiking in two cells, it could also make them to be activated more likely in random order and all the time. Thus, we predict that the role for an increased shared inhibitory input in promoting orderly and frequent R-activation of a CA3-CA3 cell pair during sharp waves is to make activation specific, in fact shared inhibition is an efficient mechanism to organize spiking in networks (when common inhibition is high network activity is more likely to organize (Bazhenov & Stopfer, 2010). Similarly, having high intrinsic excitability in the first cell of the pair could promote R-activation, but too high excitability of the second cell could harm the orderliness (and specificity) of the pair.

We next repeated the analysis for CA1-CA1 pairs, and because there are few and sparse excitatory connections between CA1 pyramidal cells, we concentrated on the excitatory inputs coming from the CA3 network and reaching both cells in the pair (Fig. 5B). We found that excitatory input significantly modulated the co-activation of CA1 neurons, i.e., CA1 pairs receiving overall larger shared excitatory synaptic inputs had higher R activation scores. Surprisingly, as shown by the small size of bars for GABA and intrinsic excitability in Fig. 5B, we found that inhibitory synaptic inputs and intrinsic excitability contributed differently to CA3 vs CA1 reactivation, in which they significantly promoted the activation of CA3 cell pairs, but not of CA1 cell pairs. We reasoned that in the case of CA1 ripple activity, the ongoing inhibitory background is so strong (because ripples are strong inhibitory events) that additional specific inhibitory synapses are not required to promote selectivity, while the shared excitability is still necessary to promote activation.

In light of these results, functionally we can suggest that reactivation during SWRs in CA3 is a network-emergent mechanism, and as such carefully regulated by excitatory and

inhibitory synapses, while in CA1 it is input-driven, and as such regulated mainly by shared CA3 synaptic projections. Our work suggests a scenario in which activation during ripples is a network-wide phenomenon, shaped by synaptic inputs differently within CA3 and CA1, and happening during events which include non-linear dynamic gating of CA3 sharp wave activity by CA1 ripples. It further suggests that careful changes in synaptic inputs preceding sleep could induce changes in the cell sequence activation seen during sleep.

#### **2.4. Connecting behavior to learning, and to spontaneous reactivation during sleep: learning a trajectory while forming a reactivation trace**

Since our study suggests that CA3 input is not only necessary for ripples to happen in the CA1 area, but it is also required for appropriate reactivation of the CA1 sequences, we next asked if awake learning could lead to repeatable patterns of CA3 reactivation during sleep. To this aim, we embedded our network model of spiking cells in a narrative of three stages: Pre-sleep, Learning Experience and Post-sleep, often used in the experimental paradigms. Just as *in vivo*, our goal was to compare spiking in Post-sleep and Pre-sleep nights in relation to the activity during the Learning Experience. We chose to tie our model Learning Experience to a paradigm of “trajectory learning” (Jones, 2012, 2015), where an animal, in an enclosure furnished with a number of feeders (in our case 8), learns to visit three selected feeder locations in a given order motivated by reward. Experimentally, a maze and, in general, spatial learning is commonly used to look for learning-related sleep reactivation, because the hippocampus has been shown to build a spatial map of environments (Kudrimoti et al., 1999; Mehta, 2015; Wilson & McNaughton, 1993), where hippocampal pyramidal cells spike at selected locations (place cells) (Davidson et al., 2009; O’Neill et al., 2006), and these cell-location code seems to persist across days unless cues in the environment are significantly changed (Davidson et al., 2009; O’Neill et al., 2006; Nitz & McNaughton, 2004; Mehta et al., 1997, 2002). Hence, *in vivo*, neurons with place fields along a trajectory spike in a specific order as an animal moves (spike sequence), and the spiking of the same cells can be observed during the sleep sessions (replay). It was shown that sequences representing learned trajectories reactivate more often in SWR in Post-sleep vs Post-sleep nights (Ji & Wilson, 2007; Kudrimoti et al., 1999; Skaggs & McNaughton, 1996; Sutherland & McNaughton, 2000; Wilson & McNaughton, 1993, 1994).

To model sleep phases (Pre-sleep and Post-sleep), we used our network of spiking CA3-CA1 neurons generating SWR complexes as described above. To model awake and learning (Learning Experience phase) we chose to model a generic spiking activity from Poisson point processes (which we interpret as the awake spiking of pyramidal cells) with rates tied to the pre-defined place fields (Place Field model) (Fig. 6A) (Malerba et al., 2017). Specifically, we constructed a virtual squared enclosure, and tiled it with the place fields, each associated with a separate Poisson process at specific location. The spiking rate of each process depended on its place field, so that at any moment in time, the position of the “virtual rat” in the enclosure would produce a distribution of the probabilities of spiking among all locations. The motion paths were straight lines connecting a feeder to the next, and an experience was then given by a list of feeders to be visited sequentially. For a specific target trajectory (list of 3 specific feeders) to be learned in a Learning Experience phase (“target trajectory”), we alternated groups of 3 random feeders with the target trajectory

multiple times that generated spiking activity in place cells. These spike trains were then used to compute the effect that a classic spike-time dependent plasticity (STPD) rule would have had on the synapses between these virtual pyramidal cells. Consistent with intuition, synapses between cells that spiked in order consistently multiple times during the Learning Experience phase would be strengthened if they favored the spiking order and weakened if they opposed it, with the strongest effect being on synapses between cells along the target trajectory. For all other cells, the random order spiking would lead to very small net synaptic changes (if at all).

The big picture of this “experiment” was constructing a Pre-sleep, Learning Experience, Post-sleep sequence, and for that we needed to introduce an explicit relationship between the synaptic changes that were calculated during the Learning Experience phase (based on Place Field model) and the actual synaptic weights of the CA3-CA1 network which simulated sleep (based on the network model of spiking CA1-CA3 neurons). To do that, we assigned each place field (and hence each awake spike train of the Place Field model) to a randomly selected pyramidal cell in the CA3 network (for a total of 81 pyramidal cells). Then, the synapses connecting the 81 cells that had place fields assigned were changed to simulate effect of learning, and the specific amount of change (in AMPA and NMDA synapses) was dictated by the Learning Experience phase. We considered the CA3-CA1 network with newly changed synapses our Post-sleep network, where the Pre-sleep network was given by the CA3-CA1 network synapses before the change was introduced.

Hence we simulated a virtual animal model with a Pre-sleep, Learning Experience, Post-sleep paradigm where we could explicitly define the relation between awake learning and synaptic changes from Pre-sleep to Post-sleep. We then tested how spiking during CA3 sharp waves was different in Pre-sleep vs Post-sleep, in particular for those cells that were given place fields associated with a target trajectory. Specifically, 7 cells with place fields along the target trajectory were selected to represent the memory spiking sequence. We found that during sharp waves the spiking sequence representing the target trajectory was reactivated more often in Post-sleep vs Pre-sleep (Fig. 6B). When we compared the gain in activation (i.e. activation in Post-sleep minus activation in Pre-sleep) of a sequence representing a target trajectory (very often experienced in the Learning phase) to a sequence representing any other random trajectory (each possibly experienced only a few times during a Learning Experience phase) we found that the target trajectory consistently showed a much larger increase in activation in the Post-sleep, compared to generic trajectories (Fig. 6C) (Malerba et al., 2017).

The simple model we presented in this section suggests a mechanism of how synaptic changes associated with repetitive sequences of cell spiking, as observed in hippocampal place cells during animal moving in a maze, can promote reactivation of the same spike sequences within sharp wave events during NREM sleep, as required for hippocampus-dependent memory consolidation.

### 3. Materials and Methods

#### 3.1. Network model: equations and parameters

We model SWR activity in the hippocampus using a network of 240 basket cells and 1200 pyramidal cells in CA3, 160 basket cells and 800 pyramidal cells in CA1. The ratio of excitatory to inhibitory neurons is known to be approximately 4 (Andersen et al., 2006) and since in our model we did not introduce any of the numerous hippocampal interneuron types but for basket cells, we apply that ratio to the pyramidal to basket cell network. This ratio also favored the ability of the network to support a background disorganized spiking regime, where excitatory and inhibitory currents were able to balance each other (Atallah & Scanziani, 2009). For each neuron, the equations are

$$C \dot{v} = -g_L(v - E_L) + g_L \Delta \exp\left(\frac{(v - V_t)}{\Delta}\right) - w + I(t)$$

$$\tau_w \dot{w} = a(v - E_L) - w$$

$$v(t) = V_{thr} \Rightarrow v(t + dt) = V_r, w(t + dt) = w(t) + b$$

$$I(t) = I_{DC} + \beta \eta_t + I_{syn}(t)$$

$$\tau d\eta_t = -\eta_t dt + dW_t$$

CA1 cells parameters are reported in (Malerba, 2016); and CA3 cells parameters were as follows. Pyramidal cells parameters:  $C$  (pF) = 200;  $g_L$  (nS) = 7;  $E_L$  (mV) = -58;  $A$  = 2;  $b$  (pA) = 40;  $\tau_w$  (ms) = 120;  $V_t$  (mV) = -50;  $V_r$  (mV) = -46;  $V_{thr}$  (mV) = 0. Interneurons parameters:  $C$  (pF) = 200;  $g_L$  (nS) = 10;  $E_L$  (mV) = -70;  $A$  = 2;  $b$  (pA) = 10;  $\tau_w$  (ms) = 30;  $V_t$  (mV) = -50;  $V_r$  (mV) = -58;  $V_{thr}$  (mV) = 0.

The coefficients establishing noise size were  $\beta = 80$  for pyramidal cells,  $\beta = 90$  for interneurons. DC inputs ( $I_{DC}$  in the equations) were selected from Gaussian distributions with mean 24 (pA) and standard deviation 30% of the mean for pyramidal cells in CA3, mean 130 (pA) and standard deviation 30% of the mean for CA3 interneurons, mean 40 (pA) and standard deviation 10% of the mean for CA1 pyramidal cells and mean 180 (pA) and standard deviation 10% of the mean for CA1 interneurons.

Synaptic currents were modeled with double exponential functions, for every cell  $n = t$  we had  $I_{syn}(t) = \sum_{j=1}^{160} g^{j \rightarrow n} s^{j \rightarrow n}(t)(v_n - E_i) + \sum_{j=1}^{800} g^{j \rightarrow n} s^{j \rightarrow n}(t)(v_n - E_e)$ , where  $E_i = -80$

mV and  $E_e = 0$  mV, and  $s^j \rightarrow n(t) = \sum_k F \left( e^{H \left( \frac{t-t_k}{\tau_D} \right)} - e^{H \left( \frac{t-t_k}{\tau_R} \right)} \right)$ , where  $t_k$  are all the spikes of pre-synaptic cell  $j$ .

In this equation,  $F$  is a normalization coefficient, set so that every spike in the double exponential within parentheses peaks at one, and  $H(\cdot)$  is the Heaviside function, ensuring that the effect of each presynaptic spike affects the post-synaptic current only after the spike has happened. The time scales of rise and decay (in ms) used in the model were as follows (Bartos, 2002; Cutsuridis et al., 2010; Malerba, 2016; Taxidis, 2012). For AMPA connections from pyramidal cells to pyramidal cells:  $\tau_R = 0.5$ ,  $\tau_D = 3.5$ . For AMPA connections from pyramidal cells to interneurons:  $\tau_R = 0.5$ ,  $\tau_D = 3$ . For GABA<sub>A</sub> connections from interneurons to interneurons:  $\tau_R = 0.3$ ,  $\tau_D = 2$ . For GABA<sub>A</sub> connections from interneurons to pyramidal cells:  $\tau_R = 0.3$ ,  $\tau_D = 3.5$ .

### 3.2. Network model: connectivity

The CA3 network was organized as a one-dimensional network. For connections from a CA3 pyramidal cell to the other CA3 pyramidal cells, we first considered a radius (of about one third of the network) around the presynaptic cell, and the probability of connection from the presynaptic cell to any cell within such radius was higher for cells with indices nearby the presynaptic cell and reduced progressively with cell index distance (Li, 1994). Specifically, we used a cosine function to shape the probability within the radius, and parameterized how fast with index distance the probability had to decay by using a monotonic scaling of the cosine phase: if  $x$  was the index distance within the network,  $y = \arctan(kx)/\arctan(k)$  imposed the decay probability  $p(y) = P \cos(4y)$ , where  $P$  was the peak probability and  $k = 2$  was a parameter controlling the decay of connection probability with distance within the radius. An analogous structure underlied the probability of CA3 pyramidal cells to connect to inhibitory interneuron in CA3 and for Schaffer Collaterals to connect a CA3 pyramidal cell to CA1 pyramidal cells (Li, 1994). To balance the relationship between feed-forward excitation from pyramidal cells to interneurons and feedback inhibition from interneurons to pyramidal cells, probability of connection from a presynaptic basket cell to a cell within a radius (about 1/3 of the network size) was constant at 0.7, for GABA<sub>A</sub> connections to both CA3 pyramidal cells and interneurons. Within CA1 connectivity was all-to-all, with the caveat that synaptic weights which were sampled at or below zero caused a removal of a given synapse. As a result, most synapses between CA1 pyramidal cells were absent, consistently with experimental findings (Deuchars & Thomson, 1996). To introduce heterogeneity among synaptic connections, synaptic weights for all synapse types were sampled from Gaussian distributions with variance ( $\sigma$ ) given by a percent of the mean ( $\mu$ ). Parameters used in the simulations were (we use the notation Py3 and Py1 to denote pyramidal cells in CA3 and CA1, respectively and analogously Int3/Int1 for interneurons). Py3  $\rightarrow$  Py3:  $\mu = 34$ ,  $\sigma = 40\% \mu$ ; Int3  $\rightarrow$  Int3:  $\mu = 54$ ,  $\sigma = 40\% \mu$ ; Py3  $\rightarrow$  Int3:  $\mu = 77$ ,  $\sigma = 40\% \mu$ ; Int3  $\rightarrow$  Py3:  $\mu = 55$ ,  $\sigma = 40\% \mu$ ; Py3  $\rightarrow$  Py1:  $\mu = 34$ ,  $\sigma = 10\% \mu$ ; Py3  $\rightarrow$  Int1:  $\mu = 320$ ,  $\sigma = 10\% \mu$ ; Int1  $\rightarrow$  Int1:  $\mu = 3.75$ ,  $\sigma = 1\% \mu$ ; Py1  $\rightarrow$  Int1:  $\mu = 6.7$ ,  $\sigma = 1\% \mu$ ; Int1  $\rightarrow$  Py1:  $\mu = 8.3$ ,  $\sigma = 1\% \mu$ ; Py1  $\rightarrow$  Py1:  $\mu = 0.67$ ,  $\sigma = 1\% \mu$ . It is to note that the mean ( $\mu$ ) declared was normalized by the total number of cells before the variance to the mean was introduced in the distribution. Since the CA3 and CA1 networks are of different

sizes, a direct comparison of the parameter values or their magnitude across regions would not account for the effective values used in the simulations.

#### 4. Discussion

Coordinated activity between hippocampal and cortical regions is believed to be critical for recent memories consolidation, and any sufficient damage to the hippocampus leads to permanent inability to form new long-term memories of facts and events. Hippocampal sharp-wave ripples are essential sleep graphoelements (characteristic events found in the ongoing electrical activity, for example as measured in LFPs or EEGs) responsible for mapping new memories from hippocampus to the permanent storage in the neocortex. It remains largely unknown what are specific intrinsic and synaptic mechanisms behind the dynamics of sharp-wave ripples in CA3 and CA1, and how their interaction can lead to layered mechanisms controlling the reactivation of sequences of pyramidal cells spikes (encoding memories) during sleep.

In this new study, using biophysical models of hippocampal CA1-CA3 network, we found that reactivation in CA3 requires fine tuning of excitatory and inhibitory synapses, which both contribute to promoting and refining spiking activity across SWR complexes. In CA1, the strong inhibitory local activity behind the ripple generation sets the pace of reactivation and only leaves a narrow window of opportunity to few pyramidal cells to spike during each ripple event. Hence, excitatory pathways from CA3 to CA1 are primarily effective at specifically shaping sequence reactivation in CA1. Data shows that reactivation is only effective for memory consolidation when happening during SWR complex, which had led to the hypothesis that SWRs could be crucial for recruiting synaptic plasticity between hippocampus and cortex (Atherton et al., 2015; Battaglia et al., 2004; Buzsaki, 2015; Euston et al., 2007; Hoffman & McNaughton, 2002; Kudrimoti et al., 1999; Sutherland & McNaughton, 2000). Our model predicts that CA1 activity can exert a form of dynamic gating over the CA3 sharp waves, which have the potential to trigger a ripple but only with some probability. In this scenario, the special role of SWR complex, as the events in which hippocampal replay happens and is broadcasted to the cortex, gains one more possible reason for its importance: CA1 ripples could selectively discard weak CA3 activity unless it was promoted (and hence made stronger) by incoming cortical or thalamic input.

We emphasize how simple manipulations of synaptic connections which can represent awake learning (such as in the “virtual rat” model) already show that there is a complex interaction between the emergent population dynamics in CA3-CA1, which makes the SWR events happen, and gating function of CA1, which selects sequences to replay. As a consequence, learning cannot just be performed by arbitrarily choosing a few synapses to strengthen and a few to weaken, but it has to be orchestrated in agreement with the structure of synaptic weights already present in the network (and possibly using neuromodulators (Atherton et al., 2015)). This implies that in the hippocampus, encoding and awake learning should happen in coordination with the reactivation in the previous sleep night, so that they can influence reactivation in the following sleep episode. This is consistent with recent data showing that the population of cells that are active during awake encoding and those that are active in the previous sleep are different in firing rate (Grosmark & Buzsaki, 2016).

We focused on how learning in CA3 can affect its ability to pattern complete during sharp waves, as our previous analysis showed that selective input to CA1 cells is effective at inducing CA1 replay during ripple (Malerba, 2016). Cutsuridis and Hasselmo (2011) have introduced a model of CA1-medial septum activity capable of learning (during theta activity) and reactivation (during ripples), where the crucial learning that enables memory replay during ripples is focused at the projections of entorhinal cortex and CA3 onto CA1 pyramidal cells, which results in a selective amount of combined entorhinal and CA3 input reaching each CA1 cell in the model during a ripple. It is possible that to obtain reactivation in the whole CA3-CA1 network, resulting in CA1 pyramidal cell sequences, selective plasticity between CA3 and CA1 pyramidal cells would also be required in our model. Furthermore, reactivation during SWRs is known to possibly happen in a reversed manner, where the trajectory is replayed from end to beginning. This is seen in quiet wake, often after receiving reward (Roumis & Frank, 2015). It is possible that to achieve reverse replay in our CA3 network we would need to explore a role for selective inhibitory synaptic weights and/or contribution of the cortical input, in addition to strengthening the excitatory connections (Chenkov et al., 2017).

While the complete picture of the continuous process of memory formation, consolidation and reconsolidation is still far from complete, it is clear that the mechanism does not start and end within the hippocampal formation, and hence this work is only addressing part of the story. Theoretical and computational models capable of connecting awake states and sleep states, and multiple structures such as cortex and hippocampus are going to be crucial in shaping hypotheses that concretely suggest how synaptic plasticity, neuromodulation and the coordination of brain rhythms can effectively enable the continuous learning and re-learning process across days and nights.

## Acknowledgements

The authors would like to thank Matt Jones for insightful discussions.

### Funding

This work was supported by the ONR (MURI N000141612829), Lifelong Learning Machines program from DARPA/MTO (HR0011-18-2-0021) and NIH (RF1 MH117155) grants to MB.

## References

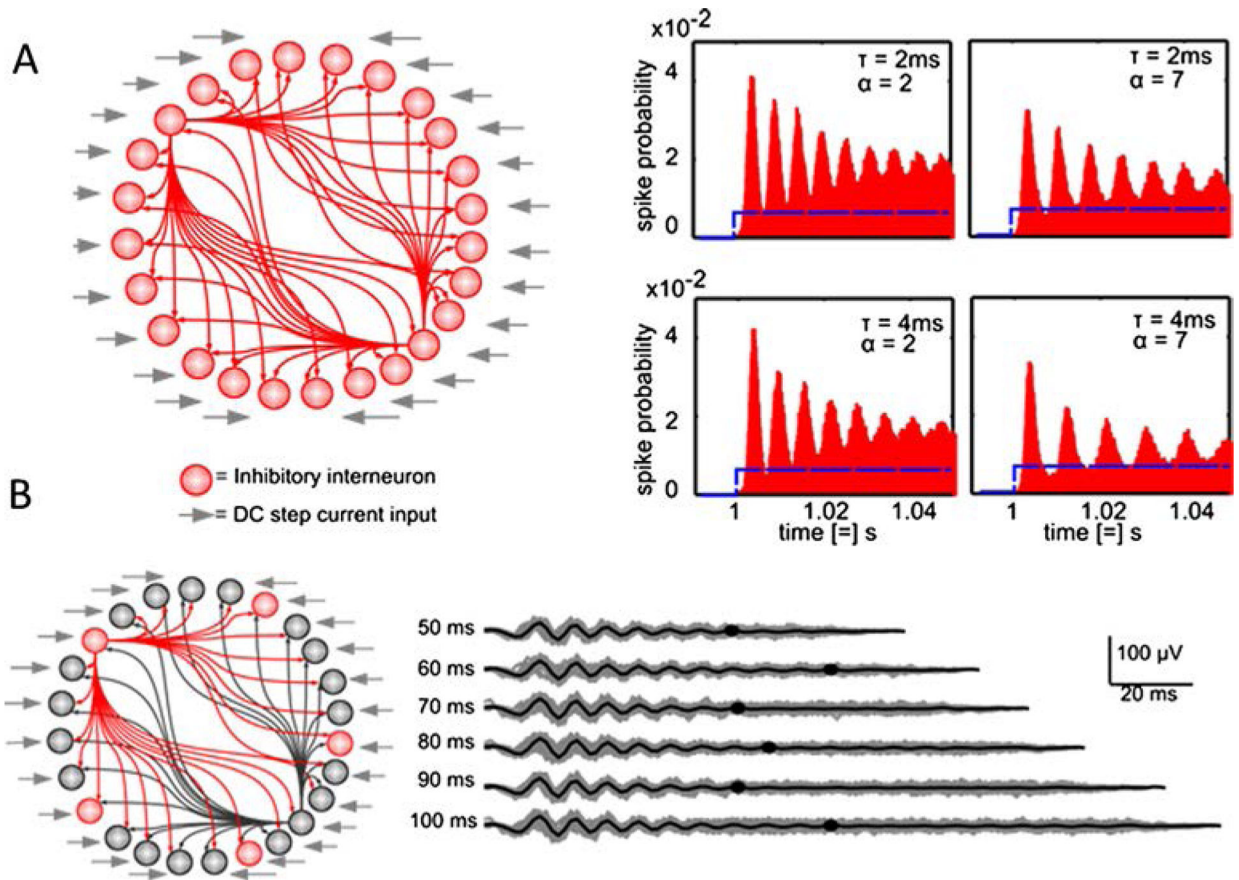
- Andersen P, Morris R, Amaral D, Bliss T, & O'Keefe J (2006). *The hippocampus book*. Oxford University Press.
- Atallah BV, & Scanziani M (2009). Instantaneous modulation of gamma oscillation frequency by balancing excitation with inhibition. *Neuron*, 62, 566–577. [PubMed: 19477157]
- Atherton LA, Dupret D, & Mellor JR (2015). Memory trace replay: The shaping of memory consolidation by neuromodulation. *Trends in Neurosciences*, 38, 560–570. [PubMed: 26275935]
- Bartos M, Vida I, Frotscher M, Meyer A, Monyer H, Geiger JR, & Jonas P (2002). Fast synaptic inhibition promotes synchronized gamma oscillations in hippocampal interneuron networks. *Proceedings of the National Academy of Sciences of the United States of America*, 99, 13222–13227. [PubMed: 12235359]
- Battaglia FP, Sutherland GR, & McNaughton BL (2004). Hippocampal sharp wave bursts coincide with neocortical “up-state” transitions. *Learning and Memory*, 11, 697–704. [PubMed: 15576887]

- Bazhenov M, & Stopfer M (2010). Forward and back: Motifs of inhibition in olfactory processing. *Neuron*, 67, 357–358. [PubMed: 20696373]
- Buzsaki G (2015). Hippocampal sharp wave-ripple: A cognitive biomarker for episodic memory and planning. *Hippocampus*, 25, 1073–1188. [PubMed: 26135716]
- Buzsaki G, Buhl DL, Harris KD, Csicsvari J, Czeh B, & Morozov A (2003). Hippocampal network patterns of activity in the mouse. *Neuroscience*, 116, 201–211. [PubMed: 12535953]
- Buzsaki G, Leung LW, & Vanderwolf CH (1983). Cellular bases of hippocampal EEG in the behaving rat. *Brain Research*, 287, 139–171. [PubMed: 6357356]
- Chenkov N, Sprekeler H, & Kempter R (2017). Memory replay in balanced recurrent networks. *PLoS Computational Biology*, 13, e1005359. [PubMed: 28135266]
- Csicsvari J, Hirase H, Czurko A, Mamiya A, & Buzsaki G (1999). Fast network oscillations in the hippocampal CA1 region of the behaving rat. *The Journal of Neuroscience*, 19, Rc20. [PubMed: 10436076]
- Csicsvari J, Hirase H, Mamiya A, & Buzsáki G (2000). Ensemble patterns of hippocampal CA3-CA1 neurons during sharp wave-associated population events. *Neuron*, 28, 585–594. [PubMed: 11144366]
- Cutsuridis V, Graham B, Cobb S, & Vida I (2010). Hippocampal microcircuits: A computational modeler's resource book. Springer Science & Business Media.
- Cutsuridis V, & Hasselmo M (2011). Spatial memory sequence encoding and replay during modeled theta and ripple oscillations. *Cognitive Computation*, 4, 554–574.
- Cutsuridis V, & Taxis J (2013). Deciphering the role of CA1 inhibitory circuits in sharp wave-ripple complexes. *Frontiers in Systems Neuroscience*, 7.
- Davidson TJ, Kloosterman F, & Wilson MA (2009). Hippocampal replay of extended experience. *Neuron*, 63, 497–507. [PubMed: 19709631]
- Deuchars J, & Thomson AM (1996). CA1 pyramid-pyramid connections in rat hippocampus in vitro: Dual intracellular recordings with biocytin filling. *Neuroscience*, 74, 1009–1018. [PubMed: 8895869]
- Diekelmann S, & Born J (2010). The memory function of sleep. *Nature Reviews. Neuroscience*, 11, 114–126. [PubMed: 20046194]
- Draguhn A, Traub RD, Schmitz D, & Jefferys JG (1998). Electrical coupling underlies high-frequency oscillations in the hippocampus in vitro. *Nature*, 394, 189–192. [PubMed: 9671303]
- Ego-Stengel V, & Wilson MA (2010). Disruption of ripple-associated hippocampal activity during rest impairs spatial learning in the rat. *Hippocampus*, 20, 1–10. [PubMed: 19816984]
- Ellenbogen JM, Payne JD, & Stickgold R (2006). The role of sleep in declarative memory consolidation: Passive, permissive, active or none? *Current Opinion in Neurobiology*, 16, 716–722. [PubMed: 17085038]
- Ellender TJ, Nissen W, Colgin LL, Mann EO, & Paulsen O (2010). Priming of hippocampal population bursts by individual perisomatic-targeting interneurons. *Journal of Neuroscience*, 30, 5979–5991. [PubMed: 20427657]
- English DF, Peyrache A, Stark E, Roux L, Vallentin D, Long MA, & Buzsáki G (2014). Excitation and inhibition compete to control spiking during hippocampal ripples: Intracellular study in behaving mice.
- Euston DR, Tatsuno M, & McNaughton BL (2007). Fast-forward playback of recent memory sequences in prefrontal cortex during sleep. *Science*, 318, 1147–1150. [PubMed: 18006749]
- Feld GB, Weis PP, & Born J (2016). The limited capacity of sleep-dependent memory consolidation. *Frontiers in Psychology*, 7, 1368. [PubMed: 27679589]
- Foster DJ, & Wilson MA (2006). Reverse replay of behavioural sequences in hippocampal place cells during the awake state. *Nature*, 440, 680–683. [PubMed: 16474382]
- Gan J, Weng SM, Pernia-Andrade AJ, Csicsvari J, & Jonas P (2017). Phase-locked inhibition, but not excitation, underlies hippocampal ripple oscillations in awake mice in vivo. *Neuron*, 93, 308–314. [PubMed: 28041883]

- Girardeau G, Benchenane K, Wiener SI, Buzsaki G, & Zugaro MB (2009). Selective suppression of hippocampal ripples impairs spatial memory. *Nature Neuroscience*, 12, 1222–1223. [PubMed: 19749750]
- Grosmark AD, & Buzsaki G (2016). Diversity in neural firing dynamics supports both rigid and learned hippocampal sequences. *Science*, 351, 1440–1443. [PubMed: 27013730]
- Hasselmo ME (1999). Neuromodulation: Acetylcholine and memory consolidation. *Trends in Cognitive Sciences*, 3, 351–359. [PubMed: 10461198]
- Hoffman KL, & McNaughton BL (2002). Coordinated reactivation of distributed memory traces in primate neocortex. *Science*, 297, 2070–2073. [PubMed: 12242447]
- Jahnke S, Timme M, & Memmesheimer RM (2015). A unified dynamic model for learning, replay, and sharp-wave/ripples. *Journal of Neuroscience*, 35, 16236–16258. [PubMed: 26658873]
- Ji D, & Wilson MA (2007). Coordinated memory replay in the visual cortex and hippocampus during sleep. *Nature Neuroscience*, 10, 100–107. [PubMed: 17173043]
- Jones B, Bukoski E, Nadel L, & Fellous JM (2012). Remaking memories: Reconsolidation updates positively motivated spatial memory in rats. *Learning & Memory*, 19, 91–98. [PubMed: 22345494]
- Jones BJ, Pest SM, Vargas IM, Glisky EL, & Fellous JM (2015). Contextual reminders fail to trigger memory reconsolidation in aged rats and aged humans. *Neurobiology of Learning and Memory*, 120, 7–15. [PubMed: 25698469]
- Kubota D, Colgin LL, Casale M, Brucher FA, & Lynch G (2003). Endogenous waves in hippocampal slices. *Journal of Neurophysiology*, 89, 81–89. [PubMed: 12522161]
- Kudrimoti HS, Barnes CA, & McNaughton BL (1999). Reactivation of hippocampal cell assemblies: Effects of behavioral state, experience, and EEG dynamics. *Journal of Neuroscience*, 19, 4090–4101. [PubMed: 10234037]
- Latchoumane CV, Ngo HV, Born J, & Shin HS (2017). Thalamic spindles promote memory formation during sleep through triple phase-locking of cortical, thalamic, and hippocampal rhythms. *Neuron*, 95(424–435), e426.
- Li XG, Somogyi P, Ylinen A, & Buzsáki G (1994). The hippocampal CA3 network: An in vivo intracellular labeling study. *The Journal of Comparative Neurology*, 339, 181–208. [PubMed: 8300905]
- Liu X, Ramirez S, Pang PT, Puryear CB, Govindarajan A, Deisseroth K, & Tonegawa S (2012). Optogenetic stimulation of a hippocampal engram activates fear memory recall. *Nature*, 484, 381–385. [PubMed: 22441246]
- Maier N, Morris G, Johenning FW, & Schmitz D (2009). An approach for reliably investigating hippocampal sharp wave-ripples in vitro. *PLoS One*, 4, e6925. [PubMed: 19738897]
- Maier N, Nimmrich V, & Draguhn A (2003). Cellular and network mechanisms underlying spontaneous sharp wave-ripple complexes in mouse hippocampal slices. *Journal of Physiology*, 550, 873–887. [PubMed: 12807984]
- Malerba P, Krishnan GP, Fellous JM, & Bazhenov M (2016). Hippocampal CA1 ripples as inhibitory transients. *PLoS Computational Biology*, 12, e1004880. [PubMed: 27093059]
- Malerba P, Tsimring K, & Bazhenov M (2017). From learning a trajectory to sleep reactivation: studying the role of synaptic plasticity in ripple sequence replay. *bioRxiv*. 10.1101/207894 (in revision).
- Marshall L, Helgadottir H, Mollé M, & Born J (2006). Boosting slow oscillations during sleep potentiates memory. *Nature*, 444, 610–613. [PubMed: 17086200]
- McDevitt EA, Duggan KA, & Mednick SC (2014). REM sleep rescues learning from interference. *Neurobiology of Learning and Memory*.
- Mehta MR (2007). Cortico-hippocampal interaction during up-down states and memory consolidation. *Nature Neuroscience*, 10, 13–15. [PubMed: 17189946]
- Mehta MR (2015). From synaptic plasticity to spatial maps and sequence learning. *Hippocampus*, 25, 756–762. [PubMed: 25929239]
- Mehta MR, Barnes CA, & McNaughton BL (1997). Experience-dependent, asymmetric expansion of hippocampal place fields. *Proceedings of the National Academy of Sciences of the United States of America*, 94, 8918–8921. [PubMed: 9238078]

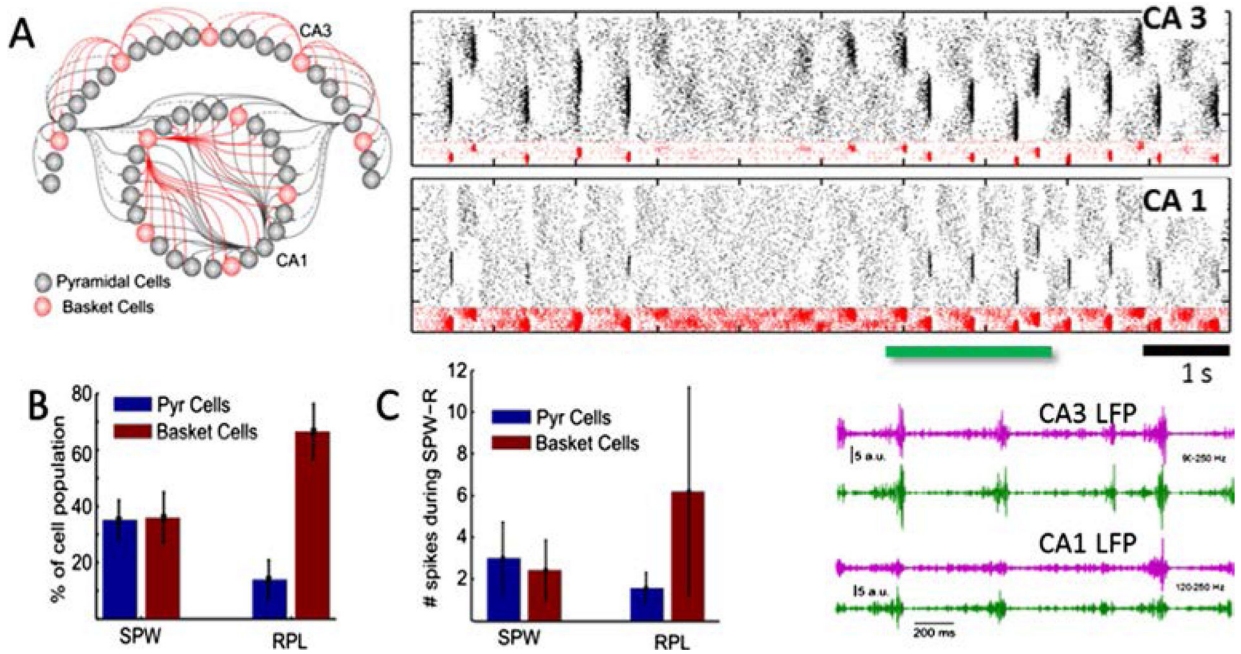
- Mehta MR, Lee AK, & Wilson MA (2002). Role of experience and oscillations in transforming a rate code into a temporal code. *Nature*, 417, 741–746. [PubMed: 12066185]
- Memmesheimer RM (2010). Quantitative prediction of intermittent high-frequency oscillations in neural networks with supralinear dendritic interactions. *Proceedings of the National Academy of Sciences of the United States of America*, 107, 11092–11097. [PubMed: 20511534]
- Mizuseki K, Royer S, Diba K, & Buzsáki G (2012). Activity dynamics and behavioral correlates of CA3 and CA1 hippocampal pyramidal neurons. *Hippocampus*, 22, 1659–1680. [PubMed: 22367959]
- Molle M, & Born J (2011). Slow oscillations orchestrating fast oscillations and memory consolidation. *Progress in Brain Research*, 193, 93–110. [PubMed: 21854958]
- Ngo HV, Claussen JC, Born J, & Molle M (2013). Induction of slow oscillations by rhythmic acoustic stimulation. *Journal of Sleep Research*, 22, 22–31. [PubMed: 22913273]
- Ngo HV, Martinetz T, Born J, & Molle M (2013). Auditory closed-loop stimulation of the sleep slow oscillation enhances memory. *Neuron*, 78, 545–553. [PubMed: 23583623]
- Nitz D, & McNaughton B (2004). Differential modulation of CA1 and dentate gyrus interneurons during exploration of novel environments. *Journal of Neurophysiology*, 91, 863–872. [PubMed: 14523073]
- O’Neill J, Senior T, & Csicsvari J (2006). Place-selective firing of CA1 pyramidal cells during sharp wave/ripple network patterns in exploratory behavior. *Neuron*, 49, 143–155. [PubMed: 16387646]
- Oliva A, Fernandez-Ruiz A, Buzsáki G, & Berenyi A (2016). Role of hippocampal CA2 region in triggering sharp-wave ripples. *Neuron*, 91, 1342–1355. [PubMed: 27593179]
- Omura Y, Carvalho MM, Inokuchi K, & Fukai T (2015). A lognormal recurrent network model for burst generation during hippocampal sharp waves. *Journal of Neuroscience*, 35, 14585–14601. [PubMed: 26511248]
- Patel J, Schomburg EW, Berenyi A, Fujisawa S, & Buzsáki G (2013). Local generation and propagation of ripples along the septotemporal axis of the hippocampus. *Journal of Neuroscience*, 33, 17029–17041. [PubMed: 24155307]
- Ramirez S, Liu X, Lin PA, Suh J, Pignatelli M, Redondo RL, Ryan TJ, & Tonegawa S (2013). Creating a false memory in the hippocampus. *Science*, 341, 387–391. [PubMed: 23888038]
- Ramirez S, Tonegawa S, & Liu X (2013). Identification and optogenetic manipulation of memory engrams in the hippocampus. *Frontiers in Behavioral Neuroscience*, 7, 226. [PubMed: 24478647]
- Rasch B, & Born J (2013). About sleep’s role in memory. *Physiological Reviews*, 93, 681–766. [PubMed: 23589831]
- Roumis DK, & Frank LM (2015). Hippocampal sharp-wave ripples in waking and sleeping states. *Current Opinion in Neurobiology*, 35, 6–12. [PubMed: 26011627]
- Schlingloff D, Káli S, Freund TF, Hájos N, & Gulyás AI (2014). Mechanisms of sharp wave initiation and ripple generation. *Journal of Neuroscience*, 34, 11385–11398. [PubMed: 25143618]
- Schwindel CD, & McNaughton BL (2011). Hippocampal-cortical interactions and the dynamics of memory trace reactivation. *Progress in Brain Research*, 193, 163–177. [PubMed: 21854962]
- Shepherd GM (2004). *The synaptic organization of the brain* (5th ed.) Oxford, New York: Oxford University Press.
- Sirota A, Csicsvari J, Buhl D, & Buzsáki G (2003). Communication between neocortex and hippocampus during sleep in rodents. *Proceedings of the National Academy of Sciences of the United States of America*, 100, 2065–2069. [PubMed: 12576550]
- Skaggs WE, & McNaughton BL (1996). Replay of neuronal firing sequences in rat hippocampus during sleep following spatial experience. *Science*, 271, 1870–1873. [PubMed: 8596957]
- Staresina BP, Bergmann TO, Bonnefond M, van der Meij R, Jensen O, Deuker L, ... Fell J (2015). Hierarchical nesting of slow oscillations, spindles and ripples in the human hippocampus during sleep. *Nature Neuroscience*, 18, 1679–1686. [PubMed: 26389842]
- Stark E, Roux L, Eichler R, Senzai Y, Royer S, & Buzsáki G (2014). Pyramidal cell-interneuron interactions underlie hippocampal ripple oscillations. *Neuron*, 83, 467–480. [PubMed: 25033186]

- Studte S, Bridger E, & Mecklinger A (2017). Sleep spindles during a nap correlate with post sleep memory performance for highly rewarded word-pairs. *Brain and Language*, 167, 28–35. [PubMed: 27129616]
- Sullivan D, Csicsvari J, Mizuseki K, Montgomery S, Diba K, & Buzsáki G (2011). Relationships between hippocampal sharp waves, ripples, and fast gamma oscillation: Influence of dentate and entorhinal cortical activity. *Journal of Neuroscience*, 31, 8605–8616. [PubMed: 21653864]
- Sutherland GR, & McNaughton B (2000). Memory trace reactivation in hippocampal and neocortical neuronal ensembles. *Current Opinion in Neurobiology*, 10, 180–186. [PubMed: 10753801]
- Taxidis J, Coombes S, Mason R, & Owen MR (2012). Modeling sharp wave-ripple complexes through a CA3-CA1 network model with chemical synapses. *Hippocampus*, 22, 995–1017. [PubMed: 21452258]
- Traub RD, & Bibbig A (2000). A model of high-frequency ripples in the hippocampus based on synaptic coupling plus axon-axon gap junctions between pyramidal neurons. *Journal of Neuroscience*, 20, 2086–2093. [PubMed: 10704482]
- Traub RD, Schmitz D, Jefferys JG, & Draguhn A (1999). High-frequency population oscillations are predicted to occur in hippocampal pyramidal neuronal networks interconnected by axoaxonal gap junctions. *Neuroscience*, 92, 407–426. [PubMed: 10408594]
- Vandecasteele M, Varga V, Berenyi A, Papp E, Bartho P, Venance L, ... Buzsaki G (2014). Optogenetic activation of septal cholinergic neurons suppresses sharp wave ripples and enhances theta oscillations in the hippocampus. *Proceedings of the National Academy of Sciences of the United States of America*, 111, 13535–13540. [PubMed: 25197052]
- Wilson MA, & McNaughton BL (1993). Dynamics of the hippocampal ensemble code for space. *Science*, 261, 1055–1058. [PubMed: 8351520]
- Wilson MA, & McNaughton BL (1994). Reactivation of hippocampal ensemble memories during sleep. *Science*, 265, 676–679. [PubMed: 8036517]
- Wu X, & Foster DJ (2014). Hippocampal replay captures the unique topological structure of a novel environment. *Journal of Neuroscience*, 34, 6459–6469. [PubMed: 24806672]
- Ylinen A, Bragin A, Nadasdy Z, Jando G, Szabo I, Sik A, & Buzsaki G (1995). Sharp wave-associated high-frequency oscillation (200 Hz) in the intact hippocampus: Network and intracellular mechanisms. *Journal of Neuroscience*, 15, 30–46. [PubMed: 7823136]



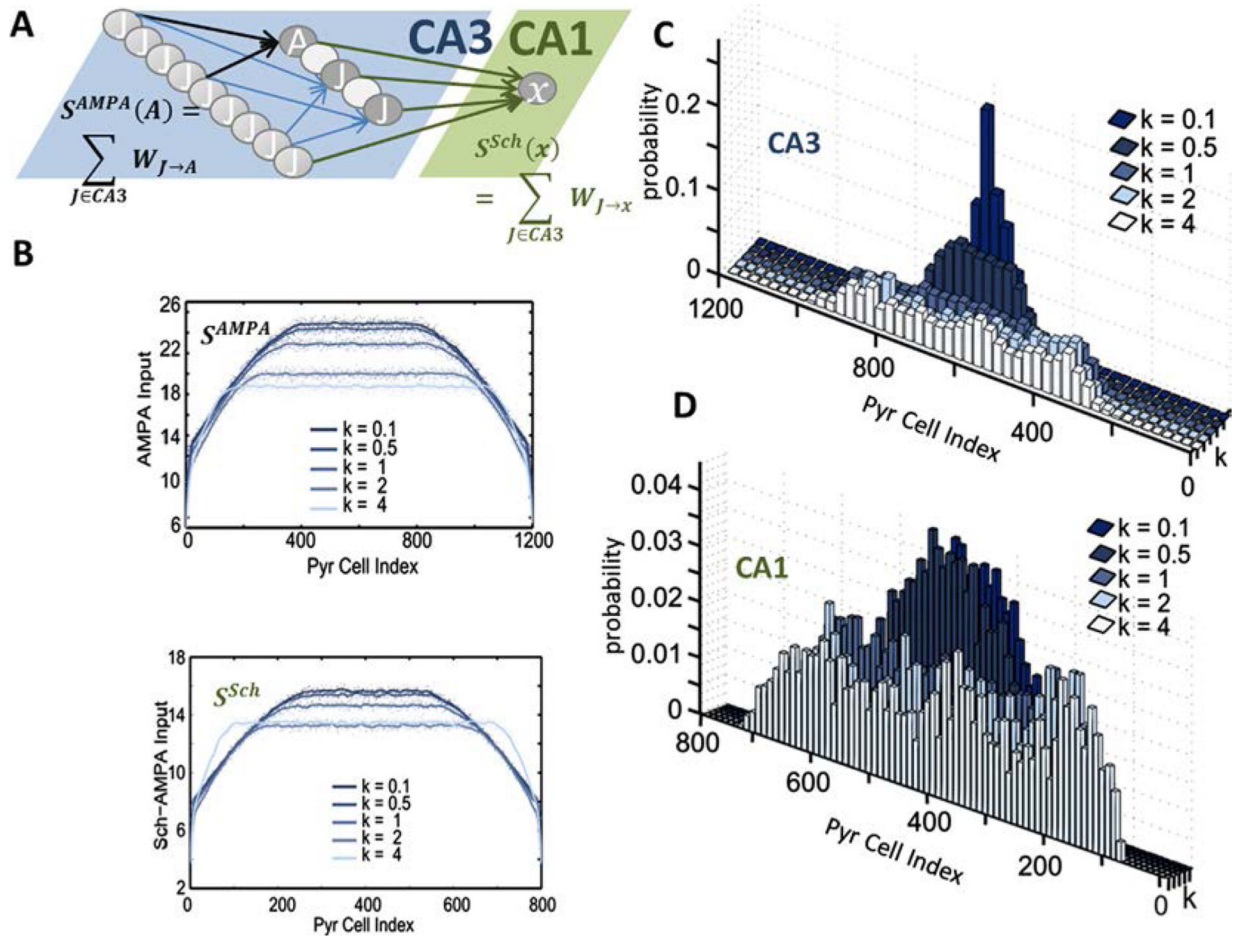
**Fig. 1.**

Ripples in CA1 are inhibitory transients. (A) Considering a small network of basket cells, with current input (representing CA3 sharp-wave activation) reaching the interneurons simultaneously. Note that the input arrives at time 1 and persists for 50 ms (time duration shown in the plots). The bar plots show that the population spikes organize in brief pulses, with inter-pulse intervals depending on the time scale of synaptic inhibition between the cells ( $\tau$ ) and the strength of synaptic connections ( $\alpha$ ). Note that activity quickly settles for an intermediate non-oscillatory firing rate. If this activity was a persistent oscillation, all peaks and trough would be the same height across time. (B) In the CA1 network of pyramidal cells and basket cells the transient behavior of CA1 ripples is shown when comparing CA3 inputs of different duration. Shown are multiple local field potentials and their average for a range of different CA3 inputs. Note how the amplitude of high-frequency oscillations in the average trace quickly decays regardless of input duration. Black dots identify the time points in which ripple detection marks the end of the ripple in the average trace (Malerba, 2016).



**Fig. 2.**

Sharp-Wave Ripple complexes in CA3-CA1 are a combination of two fundamentally different dynamics. (A) Model of CA3-CA1 network activity, where CA3 pyramidal cells project to both CA1 pyramidal and basket cells. Note that spontaneous and stochastic emergence of localized sharp waves in CA3 triggers locally organized ripples. The local field potential traces are sampled from two different locations (groups of pyramidal cells) in the network, to show that not all locations identify a ripple simultaneously (consistent with experimental data). (B and C) shows that sharp wave and ripples have fundamentally different dynamics: (1) during sharp waves (SPW) the fraction of excitatory and inhibitory cells spiking is balanced, and both populations spike only few spikes during the events; while (2) during ripples (RPL) the interneuron population dominates the event, with more cells and more spikes per ripples as compared to excitatory cells.

**Fig. 3.**

CA3 connectivity shapes SPW and RPL activity. (A) A schematic drawing representing CA3 pyramidal cells and CA1 pyramidal cells connections and how we quantify their incoming synaptic input. For CA3 cells, the total synaptic weight coming from all other CA3 pyramidal cells is summed to compute  $S^{AMPA}$ . Note that connectivity in CA3 determines the plateau shape of the convergence function over the CA3 population (Materials and Methods). For CA1 pyramidal cells, the total synaptic weights for AMPA synapses coming from CA3 cells (the Schaffer Collaterals) are summed to compute  $S^{Sch}$ . In this section, we scaled both inputs to probe possible changes in size and locations of SPW and RPL using a scaling parameter  $k$ , which controls the degree of convergence in the network. The standard network has  $k = 2$ . (B) Analysis of CA3 behavior across connection profiles. Left: AMPA input on CA3 Pyr Cells, as sum of incoming excitatory synaptic weights from other CA3 pyramidal cells. Lines mark average across 20 simulations. Input is shown for different values of parameter  $k$ , where higher values of  $k$  lower the overall amount of input. Right: AMPA input from CA3 pyramidal cells on CA1 pyramidal cells (sum of all incoming synaptic weights from Schaffer collateral, see (A)). Lines mark average across 20 simulations. (C) Distribution of SPW locations for different  $k$ . Histograms of different colors mark locations of SPWs across all CA3 pyramidal cells. Values of parameter  $k$  that lower the height of input plateau generate a wide distribution of locations. Conversely, values of  $k$

which induce higher inputs condition the SPWs to stay mostly in one central location. (D) Distribution of RPL locations for different connection profiles. Note that RPL locations are highly dependent on SPW locations. RPL distributions get less focal as the input plateau gets lower.

Author Manuscript

Author Manuscript

Author Manuscript

Author Manuscript

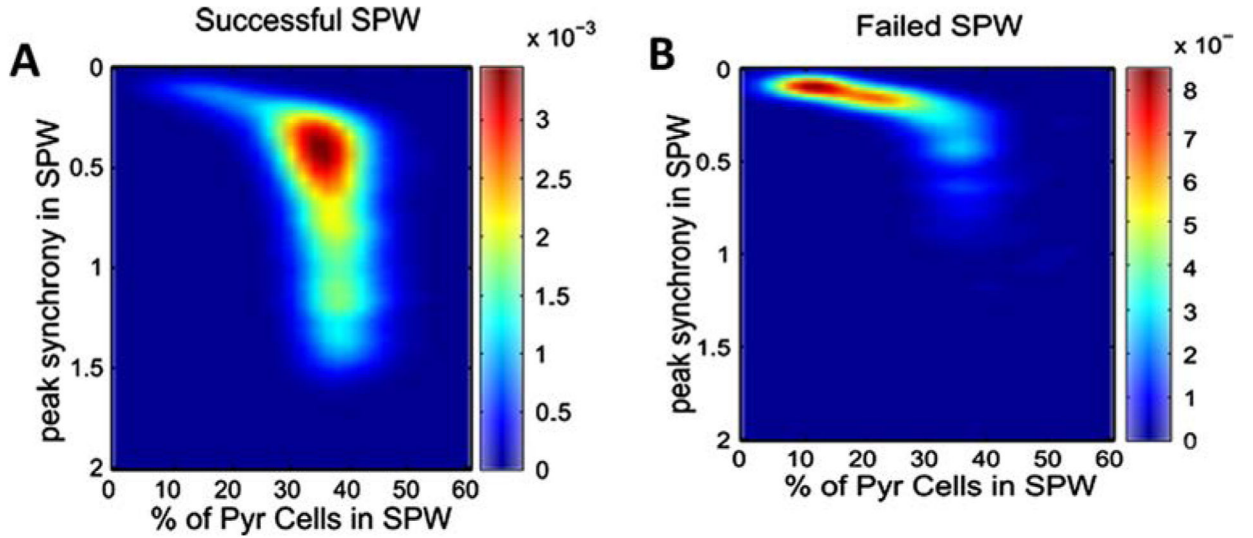


**Fig. 4.**

Nonlinear threshold in the mapping of CA3 sharp waves on CA1 ripple activity. The amount of excitatory firing in CA3 and its synchrony are different for SPWs capable of inducing a CA1 ripple (left) and those who fail (right). Looking on the pyramidal cells population spiking, all SPWs are characterized by an amount of pyramidal cells spiking during the event (SPW size) and the peak size of the probability of spiking (SPW synchrony). SPWs with more synchronized spiking will show higher peaks in CA3 spiking probability. For each SPW event in CA3, its size and synchrony are plot against each other. SPWs are separated in different groups depending on whether they triggered a corresponding RPL event in CA1 (successful SPW, left) or a RPL event was not found within 50 ms of the SPW peak (failed SPW, right). Note that failed SPWs and successful SPW occupy different regions in the size/synchrony plane, indicating that CA1 RPLs are triggered by a dynamic threshold over CA3 activity, depending on size and synchrony of the excitatory input.

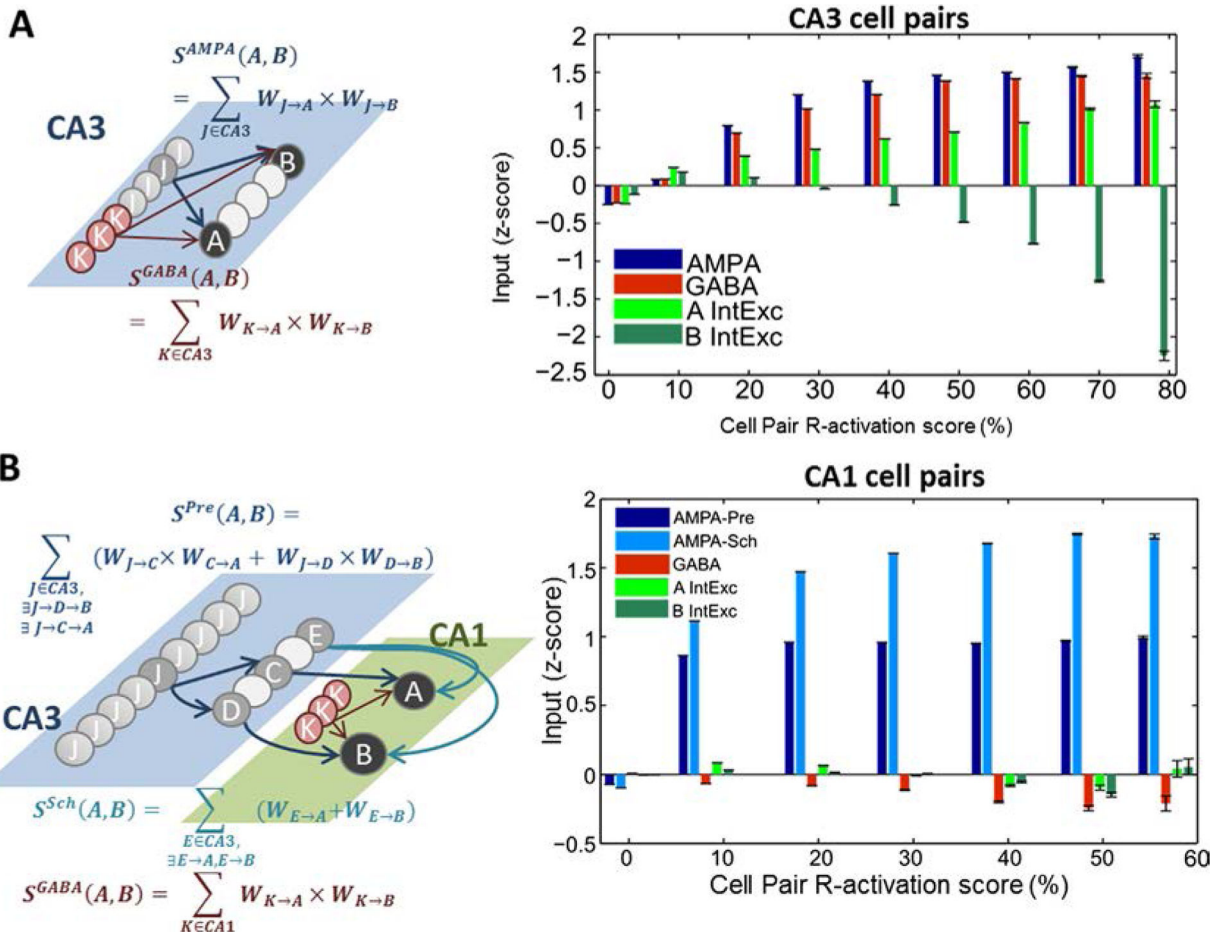


**Fig. 5.** Differential role of synaptic inputs and intrinsic excitability in promoting reactivation during SWR. (A) Relationship between activation scores during ripples and input for pairs of CA3 pyramidal cells. Left plot: drawing and formulae introduce the synaptic AMPA and GABA inputs considered ( $S^{AMPA}$  and  $S^{GABA}$ ) for any cell pair labeled (A, B). These estimates quantify the amount of excitatory and inhibitory input that cells A and B have in common. Right plot: R-activation of CA3-CA3 cell pairs is related to strength of synaptic inputs and intrinsic excitability. The bar plot shows on the x -coordinate the average R-activation score of CA3-CA3 cell pairs belonging to the same score group ( $\pm 5\%$ ) and on the y-coordinate the level of each different input ( $S^{AMPA}$ ,  $S^{GABA}$  or Intrinsic Excitability for cell A and for cell B) for cell pairs within that score group. Error bars mark the standard error of the mean. Before grouping cell pairs by their activation scores, each input was z-scored to enable comparisons of their respective trends. Therefore, a negative y-coordinate does not reflect a negative input, but an input below the average across the whole network. (B) Relationship between cell pair R-activation scores and inputs for pairs of CA1 pyramidal cells. Left plot: drawing and formulae introduce the synaptic inputs considered. For cell pair (A, B) in CA1, excitatory AMPA input from Schaffer collateral alone is labeled  $S^{Sch}$ , while the role of the excitability of presynaptic cells in CA3 is considered in defining the complementary excitatory synaptic input  $S^{Pre}$ . Inhibitory synaptic input  $S^{GABA}$  is found analogously to the

one for CA3-CA3 cell pairs (in panel A). Right plot: cell pair activation scores of CA1-CA1 cell pairs is related to strength of excitatory synaptic inputs, but not inhibitory synaptic inputs or intrinsic excitability. The bar plot shows on the x –coordinate the average activation score of CA1-CA1 cell pairs belonging to the same score group ( $\pm 5\%$ ) and on the y-coordinate the level (z-scored) of each different input (SSch, SPre, SGABA or Intrinsic Excitability for cell A and for cell B) for cell pairs within that score group. Error bars mark the standard error of the mean.

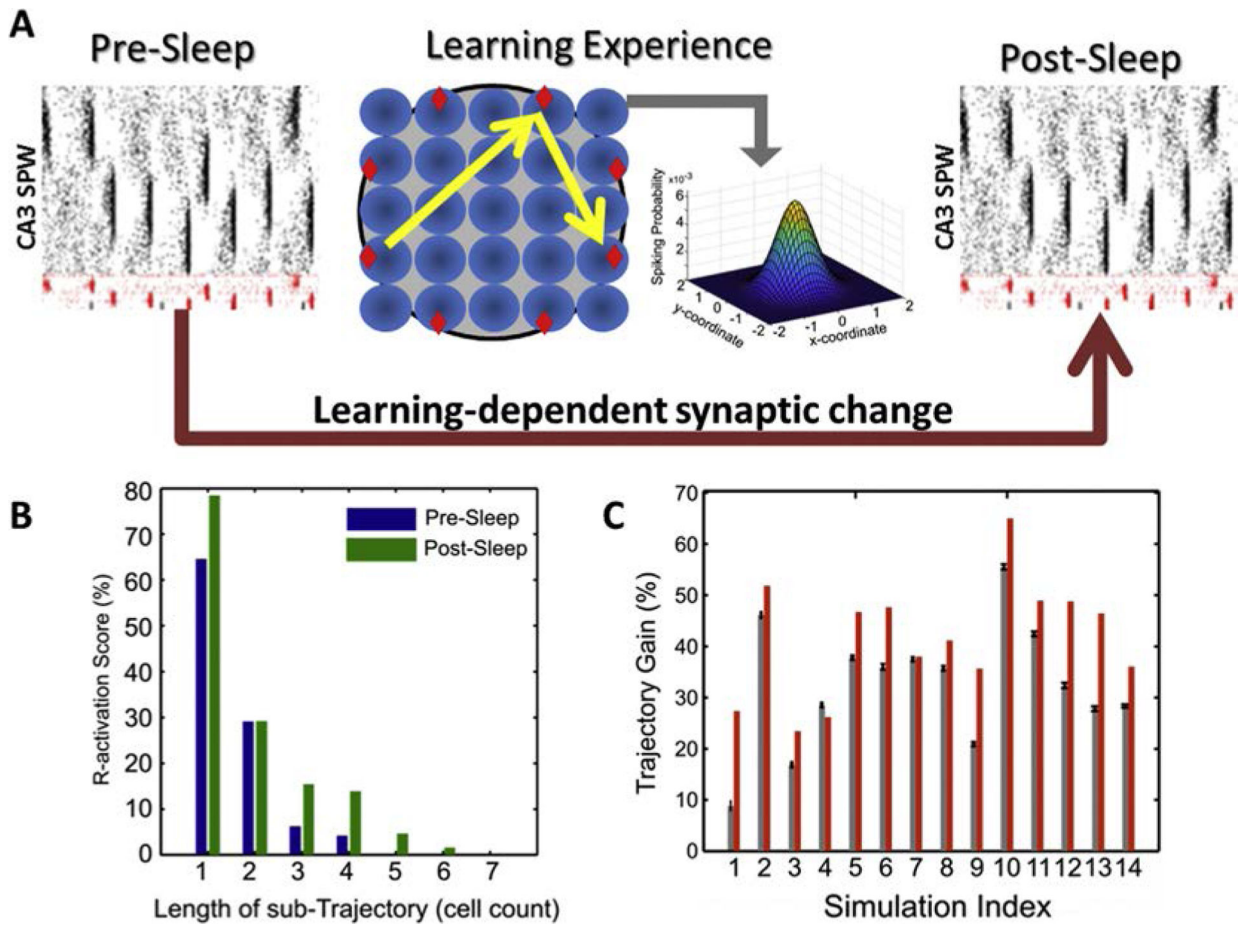


**Fig. 6.**

Learning-driven synaptic changes reflect in increased sequence activation in CA3 sharp waves. (A) A representation of the main question: we compare how changes in post vs pre sleep activity are influenced by the awake learning experience in between. The Learning Experience shows an enclosure (view from above) with 8 relevant locations (red diamonds) and a trajectory connecting 3 of them (in yellow arrows). The tiling of symmetrical place fields over the 2D enclosure is represented by blue circles, and one example of the shape of a place field is shown to emphasize that the spiking probability is highest near the center of the place field. The spiking of place cells induced by Poisson process with the fixed place fields is then unique per every different trajectory, and has some statistical variance among multiple runs of the same trajectory. We use the awake spikes to compute the effect of STDP on the synapses connecting the place cells, and assign those synaptic changes to connected cells in CA3. Then we can compare the Pre-sleep and Post-sleep spiking in the CA3 biophysical network. B. Cells which mark learned trajectories reactivate more often (in correct order) during post-sleep compared to pre-sleep. The x-axis shows sequences of cells within the trajectory of increasing lengths, bars show in percent of all ripples in which the sequences reactivated in the correct order. (C) For each simulation ( $n = 14$ ) we compare the Pre-sleep and Post-sleep activation of different trajectories. The red bar shows the Trajectory Score Gain for the learned trajectory (i.e. how the activation during post-sleep increased as compared to pre-sleep), and the gray bar shows mean and standard error of the Score Gain

for the other 336 trajectories tested, which were not learned but were possibly visited during the learning experience (Malerba et al., 2017). (For interpretation of the references to colour in this figure legend, the reader is referred to the web version of this article.)

Author Manuscript

Author Manuscript

Author Manuscript

Author Manuscript